Metrol. Meas. Syst., Vol. XX (2013), No. 4, pp. 645–654.

PAN POLSKA AKADEMIA NAUK

METROLOGY AND MEASUREMENT SYSTEMS

Index 330930, ISSN 0860-8229

www.metrology.pg.gda.pl

M&MS

FAST HIGH-IMPEDANCE SPECTROSCOPY METHOD USING SINC SIGNAL EXCITATION

Michał Kowalewski, Grzegorz Lentka

Gdansk University of Technology, Faculty of Electronics Telecommunications and Informatics, Narutowicza 11/12, 80-233 Gdansk, Poland (✉ lentka@eti.pg.gda.pl)

Abstract

In this paper the method of fast impedance spectroscopy of technical objects with high impedance ($|Z_x| \geq 1$ GΩ) is evaluated by means of simulation and a practical experiment. The method is based on excitation of an object with a sinc signal and sampling the response signals proportional to current flowing through and voltage across the measured impedance. The object's impedance spectrum is obtained with the use of continuous Fourier transform on the basis of linear approximations between samples in two acquisition sections, connected with the duration of the sinc signal. The method is first evaluated in MATLAB by means of simulation. An influence of the sinc signal duration and the number of samples on impedance modulus and argument measurement errors is explored. The method is then practically verified in a constructed laboratory impedance spectroscopy measurement system. The obtained acceleration of impedance spectroscopy in the low frequency range (below 1 Hz) and the decrease of the number of acquired samples enable to recommend the worked out method for implementation in portable impedance analyzers destined for operation in the field.

Keywords: impedance spectroscopy, sinc signal, Fourier transform, impedance analyzer.

1. Introduction

Impedance spectroscopy (IS) is a modern, advanced research tool [1], widely used in science, industry and medicine for object state testing, performance evaluation and diagnosis of different technical [2] and biological [3] objects and materials [4]. The IS consists of two phases: the object impedance measurement in a wide frequency range from mHz up to MHz and the analysis of the obtained frequency characteristic of the impedance. The collection of points describing the impedance at different frequencies of the measurement signal creates an impedance spectrum. The shape of the spectrum characterizes the structure and parameters of the tested object. Parametric identification of the object model (usually in the form of a two-terminal multi-element network) is performed on the basis of the impedance spectrum. The iterative CNLS (Complex Nonlinear Least Square) method [5] is commonly used for fitting model parameters to empirical data (the measured impedance spectrum).

In order to perform IS, instruments using SST (single sine technique) impedance measurement technique are commonly used. SST is based on excitation of the object with a harmonic signal and vector measurement of two signals: voltage across and current through the measured object. By repeating the measurements at different frequencies, the impedance spectrum can be obtained directly from measurement results as a function of frequency in a range of a few decades.

The main disadvantage of the SST technique is a very long measurement time, especially for very low measurement frequencies (mHz). The IS use in the low frequencies range is necessary in case of parametric identification of components of objects with a very high

Article history: received on Jul. 01, 2013; accepted on Oct. 28, 2013; available online on Dec. 10, 2013; DOI: 10.2478/mms-2013-0055.

impedance modulus $|Z_x| \geq 1$ GΩ. Such a situation takes place e. g. in testing high-thickness anticorrosion coatings, dielectric materials and causes that the impedance spectrum measurement lasts even a few hours and is possible only in laboratory conditions.

The need of technical diagnostics of objects located in the field also imposes meaningful time constraints. Another factor leading towards the possibility of shortening the measurement time is object changeability (especially a physico-chemical or biological one). The object changeability makes it difficult (even impossible) to fulfil the object (quasi)stationarity condition.

Due to this fact, there is need for development of alternative impedance spectrum measurement methods: much faster, dedicated for use in low-cost, miniaturized instrumentation, able to work in the laboratory as well as in the field [6-9].

Following these requirements, in order to meaningfully shorten the time of the impedance spectrum measurement (to max a few minutes) in the low frequency range (below 1 Hz), the authors have used a sinus cardinalis (sinc) signal for object excitation and signals proportional to voltage across and current through the measured impedance Z sampling with the aid of A/D converters. The paper presents results of simulations performed for different acquisition times and sampling frequencies, as well as results of the experimental verification performed in the realized measurement system.

2. Impedance measurement method

According to literature, there are proposals for shortening traditional IS by using multi-harmonic [10, 11], square pulse [12, 13] excitation or white (electrochemical) noise [14, 15].

In case of multi-harmonic signal, the tested object is excited with a signal which contains the sum of harmonic signals at frequencies selected in the range for which the spectrum needs to be determined. The method's disadvantage lies in the limitation of the measurement frequency selection. The user needs to fulfil a condition that for each component of multi-sine excitation an integer number of periods is acquired during the measurement. It can be especially difficult in the case of determining the impedance spectrum for many frequencies located in a narrow frequency range (in one decade). The problem can be solved by increasing the number of acquired periods, but this extends the total measurement time, especially for low measurement frequencies.

When using square pulse excitation, the object response signals are measured in the time domain, then their spectra are calculated with the aid of continuous Fourier transform. On the basis of impedance definition and voltage and current spectra, it is possible to determine the impedance spectrum of the tested object. Thanks to this kind of excitation, it is possible to meaningfully shorten the measurement time in relation to the SST technique but impedance spectrum determination accuracy is much worse than in the case of SST or multi-harmonic technique. The important drawbacks are also: increased calculation errors due to square pulse spectrum shape and the necessity of determination of pulse duration time depending on the measured impedance value [16].

The developed method uses a signal $u_0(t)$ of sinc (sinus cardinalis) type to excite the measured object and is aimed at measuring the impedance in the low frequency range (1 mHz ÷ 10 Hz). To determine the impedance spectrum, DSP algorithms were applied to quantized signals: $u_2(t)$ proportional to the voltage across the measured impedance Z_x and $u_1(t)$ proportional to the current through Z_x. The measurement system for implementation of the presented method is shown in Fig. 1. The system consists of a personal computer connected to a DAQ module (Agilent U2531A) [17] via an USB interface and the input circuitry developed by the Authors connecting the measured object Z_x. In the range of higher frequencies (10 Hz ÷ 1 MHz), the system uses the SST technique, measuring point by point

using a sinusoidal signal, as harmonic signals with a period lower than 100 ms influence the total IS time by a small factor.

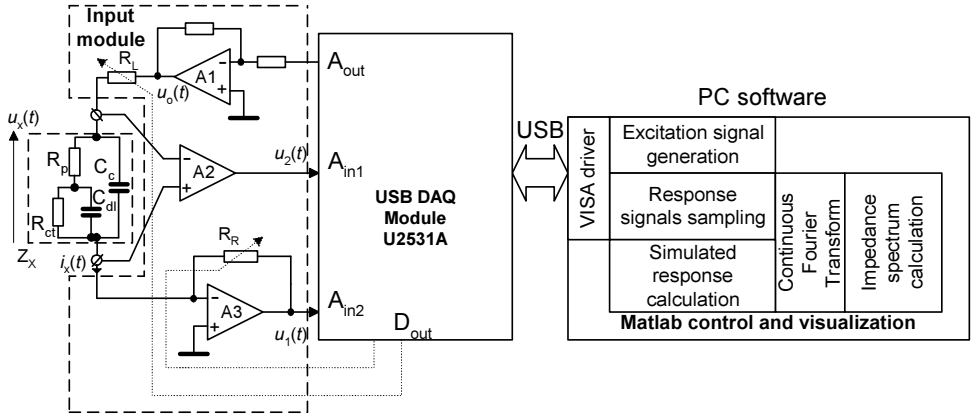

Fig. 1. Block diagram of the measurement system implementing the fast IS method.

The excitation signal for the measured Z_x is produced by a D/A converter located in the DAQ module and outputted via terminal A_{out}. In order to limit the maximum value of the current flowing through the tested object, the programmable resistor R_L was used at the output of the buffer A1 acting as source of the excitation signal $u_o(t)$. The current $i_x(t)$ is converted to voltage $u_1(t)$ in a current-to-voltage converter realized using amplifier A3. The converted current range change is realized with the aid of programmed resistor R_R. This allows to fit signal $u_1(t)$ to the measurement range of the A/D converter (input A_{in2}) located in the DAQ module. The generated excitation signal $u_o(t)$ is attenuated by the voltage divider created by resistor R_L and the measured Z_x, thus the instrumentation amplifier A2 was used in the system to measure the actual voltage $u_x(t)$ across the measured Z_x. The amplifier A2 output signal $u_2(t)$ is quantized (synchronously with u_1 (t)) by a second A/D converter (input A_{in1}) located in the DAQ module.

The collected samples of signals $u_1(t)$ and $u_2(t)$ contain information about impedance Z_x as a function of the frequency. To determine the spectrum of both signals, Fourier transformation can be used, assuming approximation of time responses with the aid of linear functions and transform calculation according to the definition:

$$U_i(j\omega) \approx \sum_{n=1}^{N-1} \int_{t_n}^{t_{n+1}} \tilde{u}_i(t) \exp(-j\omega t)\, dt\,, \tag{1}$$

where: $\tilde{u}_1(t)$ and $\tilde{u}_2(t)$ are linear approximations of each time slot of current and voltage signal of the object response.

When using above approximations and after integral calculation, one can obtain:

$$\mathrm{Re}\,U_i(\omega) \approx \sum_{n=1}^{N-1} \left[\frac{1}{\omega}\left(u_i\left(t_{n+1}\right)\sin\omega t_{n+1} - u_i\left(t_n\right)\sin\omega t_n\right) - \frac{u_i(t_{n+1}) - u_i(t_n)}{t_{n+1} - t_n} \cdot \frac{\cos\omega t_{n+1} - \cos\omega t_n}{\omega^2} \right], \tag{2}$$

$$\mathrm{Im}\,U_i(\omega) \approx \sum_{n=1}^{N-1} \left[-\frac{1}{\omega}\left(u_i\left(t_{n+1}\right)\cos\omega t_{n+1} - u_i\left(t_n\right)\cos\omega t_n\right) + \frac{u_i(t_{n+1}) - u_i(t_n)}{t_{n+1} - t_n} \cdot \frac{\sin\omega t_{n+1} - \sin\omega t_n}{\omega^2} \right]. \tag{3}$$

Using spectra of signals proportional to voltage across and current through the measured object calculated according to (2) and (3), on the basis of the impedance definition, the impedance modulus and argument spectra are calculated according to (4) for each frequency:

$$|Z_x| = \sqrt{\frac{(\mathrm{Re}\,U_2)^2 + (\mathrm{Im}\,U_2)^2}{(\mathrm{Re}\,U_1)^2 + (\mathrm{Im}\,U_1)^2}}\, R_R, \quad \varphi_{Z_x} = \mathrm{arctg}\,\frac{\mathrm{Im}\,U_2}{\mathrm{Re}\,U_2} - \mathrm{arctg}\,\frac{\mathrm{Im}\,U_1}{\mathrm{Re}\,U_1}. \tag{4}$$

One of the more important areas of the IS usage is the anticorrosion protection evaluation due to huge economic loses caused by corrosion. The IS allows determining protective features of the anticorrosion coatings on objects directly in the field, e.g. bridges, pipelines, high-voltage pylons, in order to decide whether the coating is in good or bad condition requiring renovation [18]. Thus, for the method simulation tests and experimental verification, the four-element two-terminal RC network shown in Fig. 1 (the tested object Z_x) was used. The configuration and components values are a typical example of the equivalent circuit of a high-thickness anticorrosion coating in the early stage of undercoating rusting (coating capacitance and resistance $C_c = 107.3$ pF, $R_p = 496$ MΩ, components representing undercoating rusting: double-layer capacitance $C_{dl} = 2.115$ nF and charge-transfer resistance $R_{ct} = 995$ MΩ).

3. Optimization of the method with sinc excitation

The spectrum shape of the excitation signal is an important aspect when selecting the excitation signal in the described method. The most profitable situation takes place when the excitation signal energy density is constant in the analyzed frequency range and also has as high value as possible in relation to frequencies outside the range. A sinc signal has such a feature, because the sinc signal Fourier transform is represented by a square function. Assuring a constant value of the excitation signal Fourier transform allows obtaining a similar accuracy of determination of modulus and argument of the object impedance at all measurement frequencies.

The method assumes object impedance Z_x measurement in the frequency range from f_{min} up to f_{max}, with no limitation to select specific frequencies inside the range. To achieve this condition, the sinc excitation signal parameters are regulated in a way to locate the spectrum plateau in the frequency range from f_{min} up to f_{max}.

A general form of the excitation signal used in the method expresses the following formula:

$$u_0(t) = U_0 \,\mathrm{sinc}\,(2\pi \cdot f_{max}(t - \tau)), \tag{5}$$

where: U_0 – maximum amplitude, τ – time shift, f_{max} – maximum frequency in the impedance spectrum.

Optimal selection of the total acquisition time T value is an important issue. This time should be greater than $1/f_{min}$ in order to make possible the determination of the object impedance spectrum for frequencies greater than f_{min}. Moreover, the following condition has to be fulfilled:

$$T = k\, f_{max}^{-1}, \quad (k = 1, 2, 3, \ldots). \tag{6}$$

Otherwise, at the beginning of the excitation signal ($t = 0$) there will be a voltage step which can cause rapid changes in the response signal $u_1(t)$, depending on the tested object type.

Examples of excitation signals allowing to determine the tested object impedance in a frequency range from $f_{min} = 10$ mHz covering one ($f_{max} = 0.1$ Hz), two ($f_{max} = 1$ Hz) or three ($f_{max} = 10$ Hz) decades of measurement frequencies are shown in Fig. 2 (the frequency f_{min} arises from the spectral characteristic of the tested two-terminal RC network). It was

assumed that $U_0 = 1$ V and $\tau = T/2$, hence the maximum value of $u_0(t)$ occurs in the middle of acquisition time $u_0(\tau) = 1$ V.

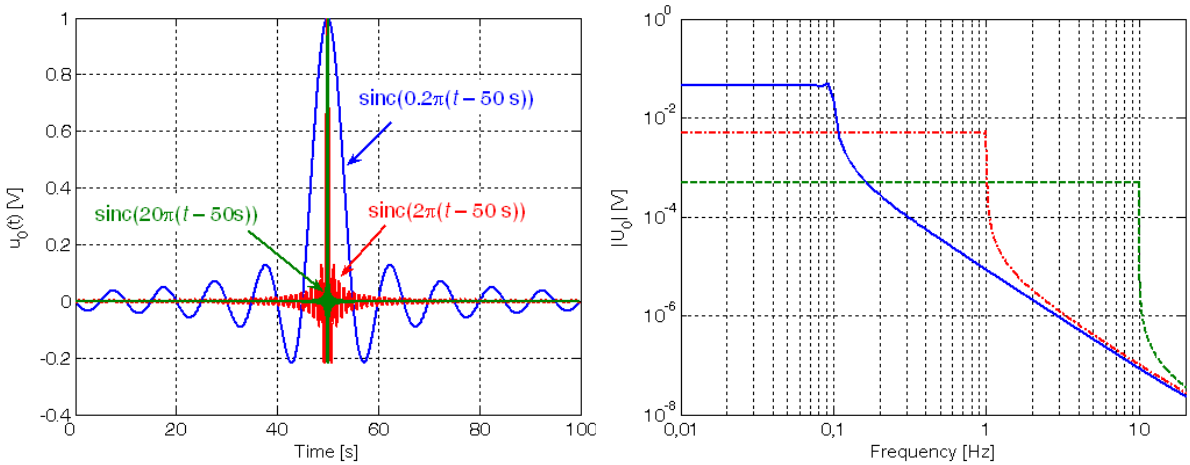

Fig. 2. Exemplary excitation signals type sinc (a), and their spectra (b).

As it is shown in Fig. 2, the sinc signal spectra shapes have the required constant value but the signal level decreases strongly with extending bandwidth. It can be supposed that this will cause a decrease of the impedance spectrum accuracy. Due to this fact, the developed method was compared by simulation means for cases $f_{max} = 0.1$ Hz and 1 Hz. For tests the four-element two-terminal RC network shown in Fig. 1 was used. The relative error of the impedance modulus and absolute error of impedance argument of the object were calculated for one (10 mHz – 100 mHz) and two (10 mHz – 1 Hz) frequency decades (at 15 frequency points logarithmically spaced in each decade) as a function of the sampling frequency of response signals $u_1(t)$ and $u_2(t)$. For both cases the sinc excitation signal with $U_o = 1$ V amplitude, duration time $T = 100$ s and excitation signal time shift $\tau_{imp} = 50$ s was used and a total acquisition time $T_{acq} = 100$ s was set.

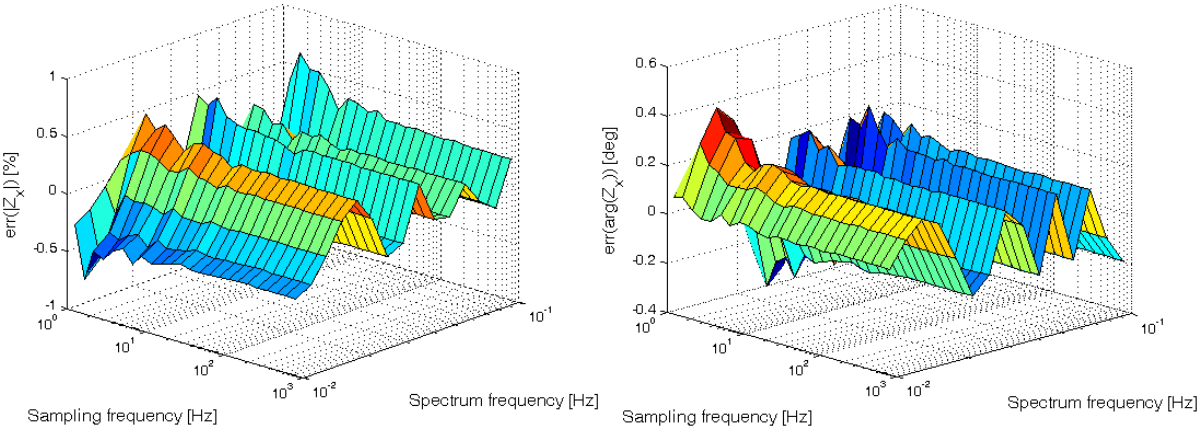

Fig. 3. Relative error of modulus and absolute error of argument of two-terminal RC network impedance in range of 10 mHz – 100 mHz.

The analysis of graphs (in Fig. 3 and 4) proves an increase of the impedance modulus and argument errors in case of extending the frequency range from one decade to two decades. A particular increase of errors can be noticed for a sampling frequency (f_s) lower than 100 Hz. Additionally, for the spectrum in the range of two decades (Fig. 4), an increase of the

impedance modulus and argument errors can also be noticed for frequencies in the lower frequency band (10 mHz – 100 mHz).

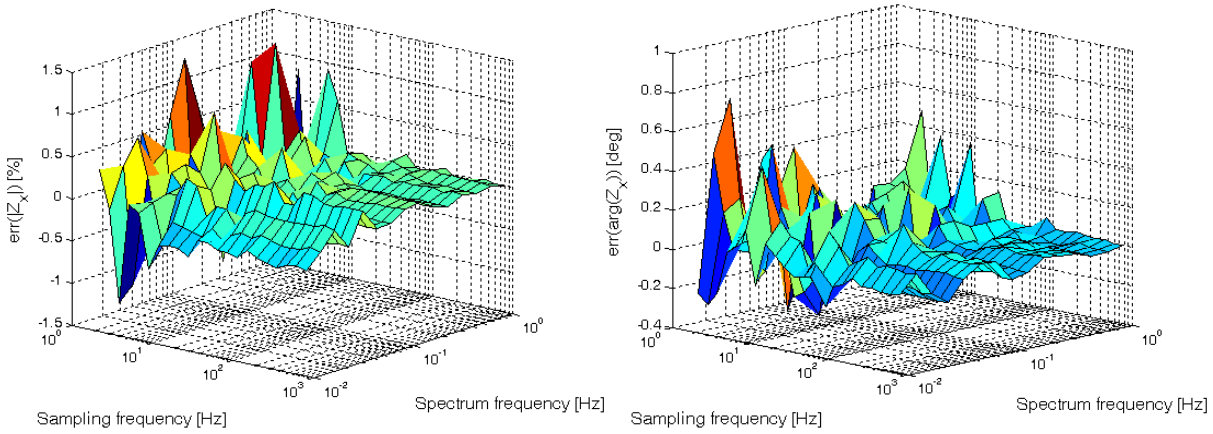

Fig. 4. Relative error of modulus and absolute error of argument of two-terminal RC network impedance in the range of 10 mHz – 1 Hz.

Taking into account the above mentioned factors influencing the accuracy of the impedance spectrum determination, the experimental verification of the method in the measurement system will be performed for one decade range for a sampling frequency f_s = 1 kHz.

4. Laboratory measurement system

The measurement system for evaluation of the developed sinc method is shown in Fig. 5. The system consists of a portable computer connected via the USB interface to the DAQ module (Agilent U2531A) and an input module developed by the Authors. The input module buffers the impulse excitation signal $u_o(t)$ and conditions the response signals proportionally to the current through $u_1(t)$ and voltage across $u_2(t)$ the measured impedance Z_x. The excitation signal $u_o(t)$ is produced using a digital-to-analog converter DAC1 located in the DAQ module. In order to limit the maximum value of current $i_x(t)$ flowing through the measured object, a programmed resistor R_L has been used at the output of buffer A9 (10 resistors 1 GΩ...1 Ω switched by reed-relays). In case of object Z_x presenting a DC potential (e.g. for electrochemical objects a chemical potential), converter DAC2 in the DAQ module allows adding a voltage compensating the object's open-circuit potential.

Extraction of the current signal $i_x(t)$ flowing through Z_x is performed using a current-to-voltage converter (amplifier A1). Using the current-to-voltage converter and ground terminal G allows to eliminate the influence of parasitic capacitance between the wire connecting terminal L and ground for shielding the object under measurement (shielding of high-impedance objects is necessary for elimination of noise induced by power lines). The obtained profit results from extortion of the almost-zero voltage between terminal L and G caused by connecting them to the input of amplifier A1. In this way, there is no current flow through these terminals, and the parasitic capacitance between them can be treated as a virtual open-circuit. To assure a wide range of the measured impedance Z_x (current i_x changes from 10 pA to 10 mA), range resistors R_R (1 GΩ, 100 MΩ, 10 MΩ...10 Ω) have been used and switched in decades by reed-relays.

Signal $u_1(t)$ proportional to $i_x(t)$ is taken from resistors R_R with the aid of voltage-followers A3 and A4 and differential amplifier A6. The range change of the converted current $i_x(t)$

obtained by resistors R_R and gain (1 or 10) of A6 allows to fit signal $u_1(t)$ to the measurement range of the analog-to-digital converter ADC1 located in the DAQ module.

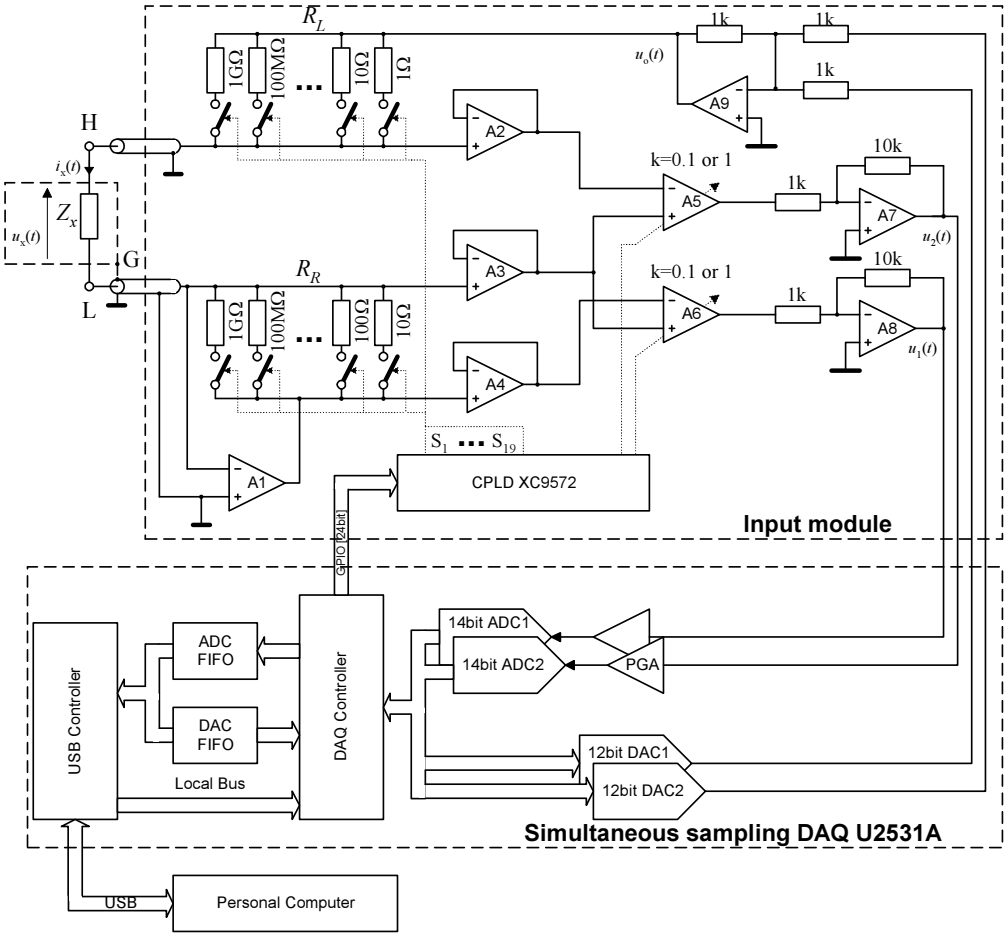

Fig. 5. Block diagram of the system for impedance spectrum measurement using sinc signal excitation.

The generated excitation signal $u_o(t)$ is not an ideal sinc signal, and additionally it is deformed by parasitic capacitance existing in parallel to resistor R_L and terminal H, so, in the presented system, a measurement channel for voltage $u_x(t)$ across Z_x was used. The path consists of voltage followers A2 and A3 and differential amplifier A5. The channel's output signal $u_2(t)$ is sampled (synchronously with $u_1(t)$) by a second analog-to-digital converter ADC2 in the DAQ module.

Full symmetry of both channels for conditioning of signals $u_1(t)$ and $u_2(t)$ leading to the same phase shift was achieved using the same number of voltage-followers and amplifiers with 1 (or 10) gain. Following the same reason, the U2531A module which allows simultaneous sampling of both signals by two analog-to-digital converters ADC1 and ADC2 working in parallel, was used.

5. Experimental results

In order to verify the simulation results, the measurements have been performed using the realised laboratory measurement system (Fig. 5). As a test engine, the reference 4-element two-terminal RC network with configuration presented in Fig. 1 was used. The reference capacitors have been measured using Precision LCR Meter E4980A, but the resistors were measured by the technical method using a precise reference resistor and a HP34401A

multimeter. The tests were performed only in the low-frequency spectrum range from 10 mHz up to 100 mHz (15 logarithmically spaced frequency points). For each frequency, a 10 measurement series was taken, and the calculated mean values were compared to values determined theoretically on the basis of reference values of the two-terminal RC network components.

Figure 6 presents the two-terminal RC network impedance modulus relative error and absolute argument error for a sinc signal with $U_o = 1$ V amplitude, duration time $T = 100$ s and excitation signal time shift $\tau_{imp} = 50$ s as a function of the sampling frequency.

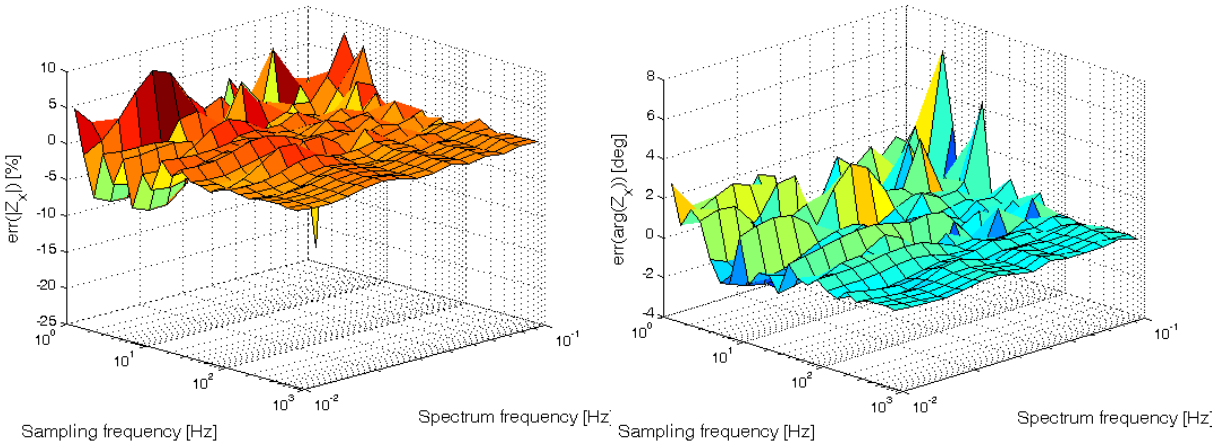

Fig. 6. Relative error of modulus and absolute error of argument of two-terminal RC network impedance.

When comparing the above-presented graphs which resulted from measurements with results obtained by simulation means (in Fig. 3), the meaningful error increase for sampling frequencies lower than 100 Hz can be noticed. In simulation tests, the impulse noise coming from DC/DC converters and quartz clocks was not taken into account. At lower sampling frequencies, this noise is not filtered well enough and it influences an increase of the impedance measurement error. In order to minimize the influence of this noise, the sampling frequency was assumed as $f_s = 1$ kHz.

The obtained results, shown in figure 6, are satisfactory. Mean values of impedance calculation errors are in the range ± 2 % for modulus and ± 1 ° for argument, while standard deviations are comparable in the entire range of measurement frequencies ($\sigma_{|Zx|} < 1$ %, $\sigma_{\arg(Zx)} < 0.6$ °).

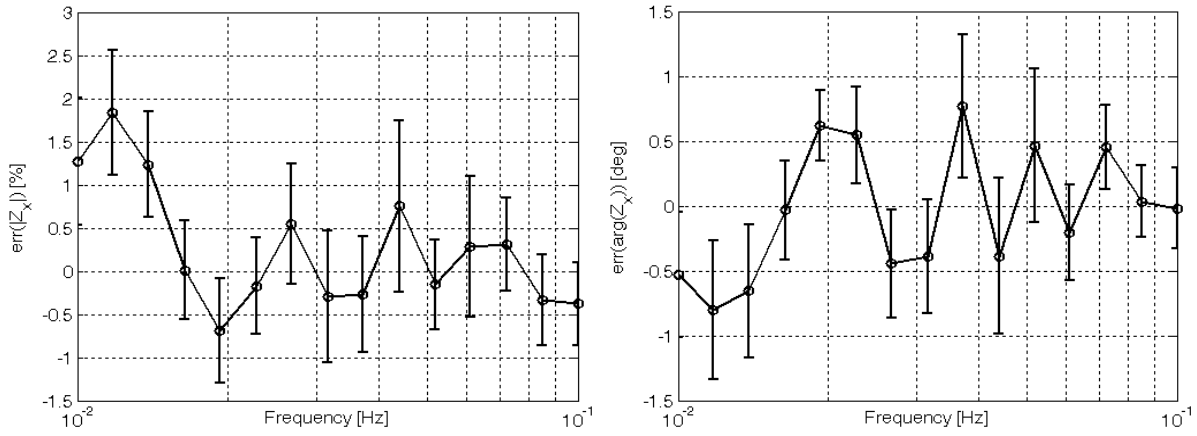

Fig. 7. Mean and standard deviation of impedance modulus (a) and argument (b) calculation errors of two-terminal RC network impedance for $f_s = 1$ kHz.

Practical experiments using the proposed method have pointed to the necessity of limiting the measurement frequency range to a maximum of 1.5 decade. When the spectrum needs to be determined in a wider frequency range, it is worth to divide this range to a few subranges and taking measurement series using sinc signals with parameters optimized for each subrange separately. The resulting impedance spectrum of the tested object is obtained by connecting results from calculation from each subrange. The total measurement time will be longer, but the error of impedance modulus and argument determination in the tested object impedance spectrum will be lower. Additionally, limiting measurement frequency range to 1.5 decade also has an advantage in decreasing excitation signal $u_0(t)$ dynamics (down to ca. 44 dB) as well as response signals $u_1(t)$ and $u_2(t)$ of the tested object. This allows to make measurements using a 12-bit ADC. Also the range resistor R_R for the $u_1(t)$ signal can be optimally selected in each measurement frequency subrange.

Resuming, the obtained impedance modulus and argument accuracy for the developed method is fully acceptable in case of the measurements in the field.

6. Conclusions

The use of impedance spectroscopy method using sinc signal excitation allows to shorten the measurement time a few times in relation to the SST technique. For example, for 15 frequency points in the 10 mHz – 100 mHz range, the measurement time for SST method is equal to ca. 600 s (assuming that the measurement at each frequency lasts only one period) while using sinc excitation the total measurement time is equal to the period of the frequency component with the lowest frequency, thus equals 100 s.

When comparing to the method using a multi-harmonic excitation signal, the measurement time is identical, but the method using a sinc signal has the advantage of free selection of measurement frequencies in the analyzed range from f_{min} up to f_{max}. The effectiveness of both methods is comparable when limiting the measurement frequencies range down to 1.5 decade.

When comparing the sinc signal excitation and square pulse excitation methods, it can be noted that much better accuracy of impedance spectrum determination is obtained for sinc signal excitation (ca. of an order better). The use of sinc signal excitation allows also free selection of the sampling frequency which additionally can be constant during response signal acquisition. In case of the square pulse excitation method, there is need to use a variable sampling frequency due to rapid changes of response signals of the tested impedance at the beginning and at the end of the square pulse.

Resuming, the method using a sinc signal, due to the following advantages:

- shortening measurement time when comparing with the SST technique,
- better accuracy of impedance determination in relation to square pulse excitation,
- more relaxed measurement frequency selection relative to multi-harmonic excitation,
- the possibility of using a constant sampling frequency,

opens new possibilities when realizing impedance measurements of high-impedance objects in shorter time.

The developed system is a prototype which has made possible experimental verification of the method using sinc signal excitation. The system has created a base for development of an impedance analyzer for fast impedance spectroscopy in field conditions.

References

[1] Barsoukov, E., Macdonald, J. R. (2005). *Impedance Spectroscopy: Theory, Experiment and Applications*, John Wiley & Sons.

[2] Skale, S., Doležek, V., Slemnik, M. (2008). Electrochemical impedance studies of corrosion protected surfaces covered by epoxy polyamide coating systems, *Prog. Organic Coat.*, (62), no. 12, 2456–2460.

[3] Zhang, Xu, Koon Gee, Neoh, Anil, Kishen (2008). Monitoring acid-demineralization of human dentine by electrochemical impedance spectroscopy, *Journal of Dentistry*, 36(12), 1005–1012. *http://www.arcoptix.com/arcspectro-nir.htm* (December 2008).

[4] Srinivas, K., Sarah, P., Suryanarayana, S. V. (2003). Impedance spectroscopy study of polycrystalline $BI_6FE_2TI_3O_{18}$, *Bulletin of Material Science*, (26), 247–253.

[5] Macdonald, J. R. (1999). *LEVM Manual v.7.11. CNLS Immittance Fitting Program*. Solartron Group Ltd.

[6] Angelini, E., Carullo, A., Corbellini, S., Ferraris, F., Gallone, V., Grassini, S., Parvis, M., Vallan, A. (2006). Handheld-impedance-measurement system with seven-decade capability and potentiostatic function. *IEEE Trans. Instrum. Meas.*, vol. 55, no. 2, Apr. 2006, pp. 436–441.

[7] Santos, J., Ramos, P. (2011) DSPIC-Based Impedance Measuring Instrument. *Metrology and Measurement Systems*. Vol. XVIII, Issue 2, pp. 185–198.

[8] Ramos, P., Janeiro, F., Radil, T. (2010) Comparative Analysis of Three Algorithms for Two-Channel Common Frequency Sinewave Parameter Estimation: Ellipse Fit, Seven Parameter Sine Fit and Spectral Sinc Fit. *Metrology and Measurement Systems*. Vol. XVII, Issue 2, pp. 255–270

[9] Hoja, J., Lentka, G. (2006). Interface circuit for impedance sensors using two specialized single-chip microsystems. *Sensors and Actuators A-physical*, Vol. 163, No. 1, 2010, pp. 191−197.

[10] Uchiyama, T., Ishigame, S., Niitsuma, J., Aikawa, Y., Ohta, Y. (2008). Multi-frequency bioelectrical impedance analysis of skin rubor with two-electrode technique, *J. of Tissue Viability*, 17(4), 110−114.

[11] Sanchez, B., Bragos, R., Vandersteen, G. (2011). Influence of the multisine excitation amplitude design for biomedical applications using impedance spectroscopy, *33rd Annual International Conference of the IEEE EMBS (Boston, USA, 30 August – 3 September 2011),* pp 3975−78.

[12] Min, M., Ojarand, J., Märtens, O., Paavle, T., Land, R., Annus, P., Rist, M., Reidla, M., Parve, T., (2012). Binary signals in impedance spectroscopy, *34th Annual International Conference of the IEEE EMBS, (San Diego, USA, 28 August - 1 September 2012),* pp 134−37.

[13] Mejia-Aguilar, A., Pallas-Areny, R. (2008). Electrical impedance measurement using pulse excitation, *Proc. of 16th IMEKO TC4 Symp. (Florence, Italy, 22-24 September 2008,),* pp 567−72.

[14] Smulko, J., Darowicki, K., Wysocki P. (1998). Digital measurement system for electrochemical noise. *Polish Journal of Chemistry*, 72(7), 1237−1241.

[15] Smulko, J., Darowicki, K., Zieliński, A. (2002). Detection of random transients caused by pitting corrosion. *Electrochimica acta*, 47(8), 1297−1303.

[16] Hoja, J., Lentka, G. (2011). Method using square-pulse excitation for high-impedance spectroscopy of anticorrosion coatings, *IEEE Transactions on Instrumentation and Measurement,* 60 957−64.

[17] U2541-90014, Agilent U2500A Series USB Simultaneous Sampling Multifunction Data Acquisition, Programmer's Reference, Agilent Technologies, Inc., 2009.

[18] Bordzilowski, J., Darowicki, K., Krakowiak, S., Krolikowska, A., (2003). Impedance measurements of coating properties on bridge structures, *Progress in Organic Coatings*, Vol. 46, 216−219.